

Absence of phase separation in the 2D Hubbard model

A. C. Cosentini,^{1,2} M. Capone,^{1,2,3} L. Guidoni,^{1,2,3} and G. B. Bachelet^{1,2}

¹*Istituto Nazionale di Fisica della Materia (INFM), Italy*

²*Dipartimento di Fisica, Università di Roma La Sapienza, Piazzale Aldo Moro 2, I-00185 Rome, Italy*

³*International School for Advanced Studies (SISSA-ISAS), I-34014 Trieste, Italy*

(December 2, 2024)

Fixed-node Green's function Monte Carlo calculations for large 2D Hubbard lattices and large interaction strengths U show no evidence of phase separation in the entire density range from empty to half filling.

PACS numbers: 71.10.Fd, 71.45.Lr, 74.20.-z

Strongly correlated electrons and holes are generally expected to play a key role in the high- T_c superconductors. Their possible instability towards phase separation (PS), initially believed to inhibit superconductivity, is attracting a lot of interest since a few different authors [1–3] have pointed out that such a tendency may in fact be intimately related to the high- T_c superconductivity. Long-range repulsive interactions may turn the PS instability into an incommensurate charge-density-wave (CDW) instability, but the very existence of a quantum critical point associated to it may be a crucial ingredient of the superconducting transition [4]. PS and/or CDW instabilities are related to a substantial reduction of the kinetic energy, which otherwise tends to stabilize uniformly distributed states; such a reduction is typical of strongly correlated electrons, both in real and model systems. PS has been experimentally observed in $\text{La}_2\text{CuO}_{4+\delta}$ [5,6], in which the oxygen ions are able to move: in the doping interval $0.01 \leq \delta \leq 0.06$ the compound separates into a nearly stoichiometric antiferromagnetic phase and a superconducting oxygen-rich phase. In generic compounds, where charged ions cannot move, the possibility of a macroscopic PS is spoiled by the long range Coulomb repulsion and should lead to an incommensurate CDW instability [7], but here the identification of charge inhomogeneities with spoiled PS is less straightforward [8]. On the theoretical side, evidence for PS has been suggested for various models of strongly correlated electrons, as the $t-J$ model [10], the three-band Hubbard model, the Hubbard-Holstein model and the Kondo model (see e.g. Ref. [4] and references therein). Despite intensive studies, even for simple models there is no general agreement on the PS boundary: for the very popular $t-J$ model, PS is fully established only at large J , but at small J (which unfortunately happens to be the physically relevant case) theoretical and numerical results are quite controversial. Given the approximate relationship linking $t-J$ and Hubbard models [9], it is for example difficult to reconcile Emery *et al.*'s [10] initial suggestion that PS occurs at *any* value of J in the $t-J$ model, with the more recent theory by Gang Su [11], according to

which the Hubbard model does not show PS at *any* value of U/t . Dagotto *et al.*'s [3] numerical results, suggesting no tendency toward PS for both the Hubbard model and the $t-J$ model below a critical value $J < J_c \sim t$, seem to be consistent with Gang Su's theory [11] and with Shih *et al.*'s [12] recent numerical results, but are at odds with another numerical study by Hellberg and Manousakis [13]. Both theoretical and numerical results focus on thermodynamical stability, which requires the energy density \mathcal{E} of an infinite system to be a convex function of the electron density n . We can write the stability condition $\chi^{-1} = \partial^2 \mathcal{E} / \partial n^2 > 0$. PS is associated with a vanishing inverse compressibility χ^{-1} ; if χ^{-1} vanishes in a given density range $n_1 < n < n_2$, the system is not stable and will separate into two subsystems with densities n_1 and n_2 . The available exact numerical results are however limited to very small systems (the behavior of the infinite 2D lattice must often be extrapolated from 4×4 lattices), and probably suffer from significant size effects. Under these circumstances the availability of a new and powerful numerical technique [14], which allows the study of (previously unfeasible) large lattice-fermion systems, provides us with a strong motivation to further investigate the Hubbard model. Whether the 2D Hubbard hamiltonian, a prototype for interacting electrons with no long-range repulsion, shows any instability towards PS, is a very interesting open question. A numerical study may also shed some indirect light on two related issues: the $t-J$ model in the physical region of small J , and the adequacy of the one-band Hubbard hamiltonian to catch the essential physics of real high- T_c superconductors.

To evaluate the ground-state energy of the Hubbard hamiltonian

$$H = -t \sum_{\langle i,j \rangle \sigma} (c_{i\sigma}^\dagger c_{j\sigma} + h.c.) + U \sum_i n_{i\uparrow} n_{i\downarrow} \quad (1)$$

we thus implemented the fixed-node Green's function Monte Carlo (FNMC) method recently proposed for lattice fermions by van Bemmelen *et al.* [14,15], which has been successfully used by Boninsegni for frustrated Heisenberg systems [16] and by Gunnarsson *et al.* for

orbitally-degenerate Hubbard models [17]. The Green's function Monte Carlo, after a sufficiently long imaginary time, projects out the “bosonic” (nodeless) ground-state component of any initial wavefunction; apart from transient estimates, which for large systems appear to be hazardous unless the initial variational wavefunction is sufficiently close to the exact one, this method is therefore not directly usable for fermions (and for any other system whose ground-state wavefunction has nodes). The FNMC [14,15] replaces the true hamiltonian by an effective hamiltonian which confines the Monte Carlo random walk within a single nodal region (a region of the configuration space where the guiding wavefunction never changes sign), and, in analogy with the continuum case [18,19], it provides an upper bound for the true ground-state energy [15]. The variational wavefunctions we use to guide the random walks and to fix the nodes are of the Gutzwiller type, being the product of a Gutzwiller factor and two Slater determinants of single-particle, mean-field wavefunctions for up- and down-spin electrons. The optimal Gutzwiller parameter and mean-field wavefunctions (whose only parameter is the staggered magnetization) are preliminarily obtained by variational Monte Carlo (VMC) runs. A few representative variational and FNMC energies are shown in Table I for the 4×4 Hubbard lattice, for which exact results [20] are available. As expected, the VMC energy is always above the FNMC energy, which in turn is slightly above the exact energy. For comparison we show the Constrained-Path Monte Carlo (CPMC) energies of Zhang *et al.* [21], which also include a larger 16×16 lattice (last row). Especially at large U 's our results appear of comparable quality as theirs.

Our numerical study proceeds in two steps: first we fix the number of electrons to a constant value N_e and vary the electron density $n = N_e/N_s$ between 0 and 1 by choosing many different square or slightly rectangular Hubbard lattices, the number of sites N_s being either $L \times L$ or $L \times (L + 1)$; for each of these lattices we perform an independent VMC run followed by a FNMC run, and obtain the corresponding ground-state energy and statistical error. This amounts to the less usual way of varying the density suggested by Ref. [13] to avoid shell effects, and we want to double-check its size dependence by repeating the whole procedure for $N_e = 16, 32$ and 128 . The corresponding three sets of data are shown in Fig. as full dots, diamonds and squares. The energies obtained for the smaller system ($N_e = 16$, full dots) are connected by thick black lines to emphasize their change of convexity as a function of the density, a finding which could optimistically be interpreted as a finite-size signal of the system's tendency towards PS instability in the thermodynamic limit. But when we repeat the same procedure with a higher number of electrons (and correspondingly larger lattices), the change of convexity found for the $N_e = 16$ -electron system just disappears : the diamonds (corresponding to $N_e = 32$) and the squares

($N_e = 128$) evidently fall on a nice, regular curve, with a constantly positive curvature (actually, almost a constant curvature). From Fig. we then conclude that the change of convexity observed at $N_e = 16$ (full dots) is an artifact of the small system, and is wiped out as the system size increases towards the thermodynamic limit. Besides their physical message, these results also seem to suggest that the less usual way of varying the density proposed by Ref. [13], which we have used up to this point, is as bad as (in fact, worse than) the more usual prescription for small systems, and as good as any other prescription for large systems: in Fig. the $N_e = 32$ and 128 data are almost exactly on the thin green line, which was, instead, obtained by varying the electron number N_e for a large, fixed 16×16 lattice.

In the second step we want to complete our numerical study by checking whether really large values of the electron-electron repulsion U can possibly yield those signals of PS which so far we haven't found at $U = 10$. Given the previous experience, we stick to a large 16×16 lattice ($N_s = 256$ sites) and vary the number of electrons N_e to yield electronic densities $n = N_e/N_s$ ranging from empty $n = 0$ to half filling $n = 1$. In Fig. we show the electronic ground-state energy per site, obtained by our FNMC runs as a function of the density. Antiperiodic boundary conditions are adopted [22] and energies are as usually in units of the hopping parameter t throughout this paper. The calculated points are shown as full dots for average densities corresponding to closed shells and as empty dots for empty shells. The associated statistical errors are always smaller than the dot size, and thus are not visible on this plot; the solid lines are three-parameter polynomial best fits of the form $-4n + an^2 + bn^3 + cn^4$. At low density, near $n = 0$, the three sets of data for $U = 10, 20$, and 40 correctly recover the expected behavior $\mathcal{E} = -4n$, also found for the noninteracting case $U = 0$ (lower dashed curve in Fig.) and for the fully spin-polarized case (upper dashed curve). Close to half filling, near $n = 1$, they also display a reasonable trend: for larger U the curves are closer, but always below, the fully spin-polarized energy (ferromagnetic, upper dashed curve); the fact that slightly above $3/4$ filling the $U = 40$ curve almost touches the ferromagnetic curve is probably due the variational nature of our FNMC energies, which always fall slightly above the exact energy (see Table I). Finally, at half filling $n = 1$, the ground-state energy per site turns out to be proportional to $J = 4t^2/U$, with a slope -1.131 ± 0.013 which is in good agreement with the $S = 1/2$ quantum Heisenberg antiferromagnet [23]. Between $n = 0$ and $n = 1$ we observe a constantly positive curvature. Neither a change of convexity, which could in fact occur for finite systems like ours, nor a flattening of the energy-vs-density curve, which could also be taken as the hint of a phase separation in the truly infinite system, are compatible with our numerical results.

The absence of any hint of PS in our large, but finite

16×16 lattice, is in principle not enough to rule out PS in the infinite system. However the results obtained here leave little room to the expectation that major qualitative changes in the energy-vs-density curve may occur for lattice sizes larger than those considered here. On the contrary, they suggest that only for really small systems (see Fig. , thick black line) an artificial change of convexity may be observed. The comparison of Figs. and and the $U = 40$ results for a smaller 12×12 lattice (shown in Fig. as empty triangles), all indicate that even for medium-sized systems (smaller than our largest 16×16 lattices) all the energies nicely fall on the same curve, whose curvature is unambiguously positive all the way thru between empty and half filling. Our results seem thus to confirm those predictions [11,3] which rule out PS in the Hubbard model. By the same token, given the kinship between the Hubbard and $t-J$ models [9], they strengthen the hint [3] that in the physically relevant region, below some critical J_c , PS won't occur in the $t-J$ model either. Finally, if the theories linking PS, CDW instabilities and high- T_c superconductivity [1-4] must be taken seriously, then our results simply confirm that the one-band Hubbard hamiltonian is unable to catch the essential physics of these materials [24].

We thank M. Boninsegni, S. Sorella, O. Gunnarsson and M. Grilli for useful suggestions and a critical reading of this manuscript, and A. Filippetti for his precious help. GBB gratefully acknowledges partial support from the Italian National Research Council (CNR, Comitato Scienza e Tecnologia dell'Informazione, grants no. 96.02045.CT12 and 97.05081.CT12), the Italian Ministry for University, Research and Technology (MURST grant no. 9702265437) and INFM Commissione Calcolo.

[1] M. Grilli, R. Raimondi, C. Castellani, C. Di Castro, and G. Kotliar, Phys. Rev. Lett. **67**, 259 (1991); C. Di Castro and M. Grilli Physica Scripta T **45**, 81 (1992), and reference therein.
[2] V.J. Emery, and S.A. Kivelson, Physica C **209**, 597 (1993).
[3] E. Dagotto, A. Moreo, F. Ortolani, D. Poilblanc and J. Riera, Phys. Rev. B **45**, 10741 (1992).
[4] C. Castellani, C. Di Castro, M. Grilli, Phys. Rev. Lett. **75**, 4560 (1995).
[5] J.D. Jorgensen, B. Dabrowski, Shiyon Pei, D.G. Hinks, L. Soderholm, B. Morosin, J.E. Schirber, E.L. Venturini, and D.S. Ginley, Phys. Rev. B **38**, 11337 (1988).
[6] F.C. Chou *et al.*, Phys. Rev. B **54**, 572 (1996).
[7] J.M. Tranquada, B.J. Sternleb, J.D. Axe, Y. Nakamura, and S. Uchida, Nature **375**, 561 (1995).
[8] A. Bianconi, N.L. Saini, A. Lanzara, M. Missori, T. Rossetti, H. Oyanagi, H. Yamaguchi, K. Oka, and T. Ito, Phys. Rev. Lett. **76**, 3412 (1996).
[9] The $t-J$ model at small J (with $J = 4t^2/U$) does not exactly reproduce the Hubbard model in the large- U limit, but the difference between the models is much more relevant on spectral properties than on their ground-state energies (the relevant quantity for PS).
[10] V.J. Emery, S.A. Kivelson, H.Q. Lin, Phys. Rev. Lett. **64**, 475 (1990).
[11] Gang Su, Phys. Rev. B **54**, R8281 (1996).
[12] C.T. Shih, Y.C. Chen and T.K. Lee, cond-mat/9705156.
[13] C.S. Hellberg and E. Manousakis, Phys. Rev. Lett. **78**, 4609 (1997).
[14] H.J.M. van Bemmel, D.F.B. ten Haaf, W. van Saarloos, J.M.J. van Leeuwen, G. An, Phys. Rev. Lett. **72**, 1442 (1994).
[15] D.F.B. ten Haaf, H.J.M. van Bemmel, J.M.J. van Leeuwen, W. van Saarloos, and D.M. Ceperley, Phys. Rev. B **51**, 13039 (1995).
[16] M. Boninsegni, Phys. Rev. B **52**, 15304 (1995); Phys. Lett. A **216**, 313 (1996).
[17] O. Gunnarsson, E. Koch, and R.M. Martin, Phys. Rev. B **54**, R11026 (1996); *ibid.* **56**, 1146 (1997); F. Aryasetiawan, O. Gunnarsson, E. Koch, and R.M. Martin, Phys. Rev. B **55**, 10165 (1997).
[18] J.B. Anderson, J. Chem. Phys. **63**, 1499 (1975).
[19] D.M. Ceperley, Physica B **108**, 875 (1981).
[20] A. Parola, S. Sorella, S. Baroni, R. Car, M. Parrinello, and E. Tosatti, Physica C **162-164**, 771 (1989); A. Parola, S. Sorella, M. Parrinello, and E. Tosatti, Phys. Rev. B **43**, 6190 (1991).
[21] Shiwei Zhang, J. Carlson, and J.E. Gubernatis, Phys. Rev. Lett. **74**, 3652 (1995).
[22] Different boundary conditions yield energies within an error bar for 16×16 lattices and within at most two error bars for our smallest lattices; all results presented here refer to antiperiodic boundary conditions.
[23] Q.F. Zhong and S. Sorella, Euro. Lett. **21**, 629 (1993); M. Calandra and S. Sorella, Phys. Rev. B, in print.
[24] see e.g. B.J. Alder, K.J. Runge, and R.T. Scalettar, Phys. Rev. Lett. **79**, 3022 (1997), and references therein.

size	N_e	n	U	VMC	FNMC	CPMC	EXACT
4×4	10	0.625	4	-1.211(2)	-1.220(2)	-1.2238(6)	-1.2238
4×4	10	0.625	8	-1.066(2)	-1.086(2)	-1.0925(7)	-1.0944
4×4	14	0.875	8	-0.681(2)	-0.720(2)	-0.728(3)	-0.742
4×4	14	0.875	12	-0.546(2)	-0.603(2)	-0.606(5)	-0.628
16×16	202	0.789	4	-1.096(2)	-1.107(5)	-1.1193(3)	-

TABLE I. Ground-state energy per site (in units of the hopping parameter t) for a 4×4 Hubbard lattice and various values of U . N_e is the number of electrons and n is the corresponding average density. VMC: variational Monte Carlo, this work; FNMC: Fixed-Node Green's function Monte Carlo, this work; CPMC: Constrained-Path Monte Carlo, Ref. [21]; EXACT: exact diagonalization results, Ref. [20].(see text)

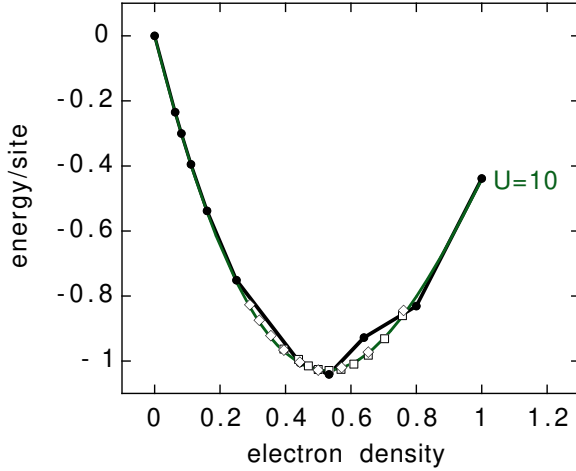


FIG. 1. (color) Ground-state energy per site (in units of the hopping parameter t) as a function of the electronic density, for finite 2D Hubbard lattices at $U=10$. The electronic density is varied by keeping the number of electrons N_e constant and varying the size of the lattice. Full dots and thick solid line: $N_e=16$; diamonds: $N_e=32$; squares: $N_e=128$. The polynomial best fit of the $U=10$ data of Fig. (see text) is shown for comparison as a thin solid green line.

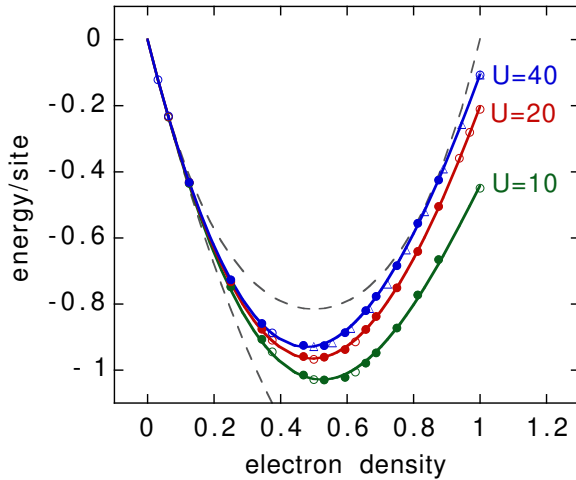


FIG. 2. (color) Ground-state energy per site (in units of the hopping parameter t) as a function of the electronic density, for a 2D Hubbard lattice of $N_s = 16 \times 16 = 256$ sites with $U = 10$ (lower, green), 20 (middle, red), and 40 (upper data, blue). The electronic density varies from 0 to 1 as the number of electrons N_e is varied from 16 to 256. Errors are smaller than the dot size. Full dots correspond to closed shells and empty dots correspond to empty shells. The solid curves which connect calculated points are three-parameter polynomial fits (see text). The dashed curves represent, instead, known analytical results: the upper one is the fully spin-polarized (ferromagnetic) energy, which is symmetric with respect to quarter filling; the lower one is the $U = 0$ noninteracting energy. The empty blue triangles, obtained for a smaller 12×12 lattice and $U = 40$, are shown for comparison (see text).